40. PETROGRAPHY AND GEOCHEMISTRY OF VOLCANIC GLASS: LEG 57, DEEP SEA DRILLING PROJECT

Kantaro Fujioka and Toshio Furuta, Ocean Research Institute, University of Tokyo, Nakano, Tokyo Japan
and
Fusao Arai, Department of Geology, Gunma University, Maebashi, Japan

ABSTRACT

About 200 volcanic ash layers were recovered during DSDP Leg 57. The volcanic glass in some of these layers was investigated petrographically and chemically in this study. Volcanic glass is mainly rhyolitic and/or rhyodacitic in chemical composition, and its refractive index ranges from 1.496 to 1.529. Some volcanic ash layers consist of multiple grains of different chemical compositions. All the volcanic glass belongs to the tholeiitic and the calc-alkalic volcanic rock series, in SiO_2–($Na_2O + K_2O$) diagram and FeO*/MgO–SiO_2 diagram. We correlated successfully three volcanic ash layers from the standpoint of chemical composition and biostratigraphy. Hydration of volcanic glass from Leg 57 is less intense than in other DSDP cores.

INTRODUCTION

Volcanic glass occurs in distinct ash layers, small pods or pockets, and as dispersed minor constituents of sediments and sedimentary rocks in the cores of DSDP Leg 57. They range in age from lower Miocene to Recent and differ from one another in various respects. Chemical composition is mainly rhyolitic and/or rhyodacitic, dacitic, and, infrequently, basaltic. Grains are typically silt-sized.

Investigation of volcanic ash has been very fruitful and provides a great deal of information about the volcanicity of source regions, chemical composition of a single volcano, hydration under conditions of burial, and so on. Because the study of volcanic ash is only beginning, many problems remain unsolved. In the present chapter we present fundamental data on volcanic ash: description, grain-size measurements, type of glass, mineralogy and chemical composition of glass shards, as well as a short preliminary discussion of original magma and alteration.

I. DESCRIPTION OF VOLCANIC GLASS

Visual Description

During Leg 57 more than 200 volcanic ash layers were identified by visual observation of the cores. A small number of ashy pods or pockets and minor amounts of dispersed volcanic glass were also distinguished in sediments and sedimentary rocks. The ash derives chiefly from the nearby Japanese Islands, transported by prevailing westerlies. Active Quaternary volcanoes, distributed west of the volcanic front of Honshu—the main land mass—supply a tremendous amount of volcanic ash to the area of the Japan Trench. Machida and Arai (1976) have summarized the distribution of typical Quaternary Japanese tephras, mapping several tephras which might have been able to reach Leg 57 sites. For example, the distribution of the tephra To-HP (Hachinohe pumice of Mt. Towada) and $Spfa_1$ (Mt. Shikotsu pumice fall) have a local distribution pattern large enough to include all sites. It is possible to identify both of these tephras at Leg 57 sites.

In the Pliocene and Miocene volcanic activity in the Japanese Islands was intense, judging from the volcanic and pyroclastic rocks and from the dispersed constituents in the sediments on land. All the volcanic ash layers and ashy pods or pockets obtained during Leg 57 are described in Table 1, with short remarks on each layer observed onboard. Ashes in Hole 436, Leg 56, are also listed in the table. At Sites 438 and 439 at the deep sea terrace, 132 distinct ash layers were distinguished throughout the recovered sedimentary column. The thickest ash layer occurs at Site 438, Core 438-11,CC and is over 16 cm. However, layers are usually less than 5 cm thick.

At Site 440, on a sedimentary pond at the trench slope bench, 57 ash layers were identified, the thickest of which is 10 cm. The difference in number of ash layers observed at Sites 438 and 439 and at Site 440 depends chiefly on time of deposition, even though Sites 438 and 439 are closer to the continent. Sites 438 and 439 penetrate lower Miocene and Site 440, upper Miocene. At Site 436, on the Pacific ocean floor, 57 ash layers were identified. Both Sites 440 and 436 are similar in number of ash layers and in sediment age. Debates concerning methods of estimating the volcanicity of regions are common. Kennett and Thunell (1975) demonstrated that the volcanic ash in deep sea sediments indicate very high rates of explosive volcanism during the last two million years. Ninkovich and Donn (1976) and Hein and Scholl (1978) have proposed a model based upon movement of the oceanic plate. Because of drilling disturbance, bioturbation, recovery rate, and many other factors, it is very difficult to record all the volcanicity in

TABLE 1
Volcanic Ash, DSDP Leg 57

Sample (Interval in cm)	Thickness (cm)	Smear Slide (cm depth)	Layer Number	Remarks	Age	SiO_2 (%)	ΣFe_2O_3 (%)	Index
Hole 438								
1-1, 62–67	5			pod, coarse pumiceous sand	upper Pleistocene			
1-1, 89–100	11			pod, coarse pumiceous sand				
1-2, 10–15	5			pod, 5Y4/1, coarse pumiceous sand				
1-2, 20–24	4			pod, 5Y4/1, coarse pumiceous sand				
1-2, 68–73	5			pod, 5Y4/1, coarse pumiceous sand				
2-3, 102–105	3			pod, white-light gray				
2-3, 128–132	4			pocket				
2-4, 122–125	3	123		pod, white gray				
2-5, 21–32	11		001	layer, multiple sandy, light gray				
2-5, 56–57	1			pocket, small				
2-5, 106–111	5	110	002	layer, light gray-white		76.45	2.06	1.502–1.506
2-6, 24–26	2			pod				
2, CC, 5–6	1			pocket, gray-white				
3-1, 86–88	2			pocket				
3-2, 15–26	11			pocket, pumiceous				
3-6, 91–98	7	96	003	layer, gray-white				
7-2, 48–50	2	49	004	layer, 5B6/1, medium-grained	upper Pliocene			
7-2, 103–105	2	104	005	layer, 5B6/1, medium-grained				
7-7, 2–5	3	3	006	layer, 5Y3/2, medium-grained		75.48	1.47	1.500–1.506
8-3, 2–4	2			pocket, black				
8-3, 3–7	4			pocket, white				
8-3, 7–11	4			pocket, white				
8-4, 43–49	6			pocket, black				
8-4, 70–73	3			pocket, black				
8-4, 74–83	9			pocket, black				
8-4, 81–82	1			pocket, small				
8-4, 83–86	3			pocket				
8-4, 95–97	2			pocket, small				
8-4, 100–104	4			pocket				
8-4, 114–117	3			pocket				
8-5, 11–15	4			pocket				
8-7, 9–12	3		007	layer, N6-N4, fine-grained, gray		77.40	1.48	
10-4, 17–24	7	23	008	layer, 5Y5/1, fine-grained, gray				
10-5, 17–22	5		009	layer, 5Y3/1, fine-grained, gray				
10-5, 81–83	2	82	010	layer, N5-N3, fine-grained		78.21	1.37	
10-6, 20–25	5	23	011	layer, 5B7/1, silty				
10-6, 25–33	8	27	012	layer, 5Y3/1, fine				
11-1, 9–16	7		013	layer, 5Y2/1, fine				
11-1, 31–36	5		014	layer, N4-N5, medium-grained				
11-1, 41–45	4		015	layer, N4, medium-grained				
11-3, 29–36	7		016	layer, N4, coarse-grained				
11-3, 88–94	6		017	layer, N4, sandy				
11-3, 125–131	6		018	layer, 5B6/1–5Y3/1, sandy				
11-4, 58–65	7		019	layer, 5B6/1, medium-grained				
11-4, 83–95	12		020	layer, 5B6/1, medium-grained				1.506–1.508
11-4, 111–115	4		021	layer, 5B6/1, medium-grained				
11-5, 26–32	6		022	layer, 5B6/1, medium-grained				
11-5, 106–111	5		023	layer, 5B7/1, medium-grained				
11, CC, 4–20	16		024	layer, 5B6/1, silty				
12-5, 60–61	1	61		layer, ashy sand				
Hole 438A								
2-2, 104–106	2			pocket	upper Pleistocene			
2-2, 122–129	7	124	025	layer, 5G4/1				
2-3, 24–27	3			pocket, 5G4/1				
2-3, 51–55	4			pocket				
2-4, 119–120	1		026	layer				
2-4, 130–134	4		027	layer, 5G4/1		78.41	1.19	
2-5, 15–23	8	21	028	layer, 5B7/1, silty				1.502–1.503
2-5, 32–35	3			pocket				
2-5, 42–48	6			pocket				
2-6, 105–110	5			pocket, 5G4/1				
3-2, 116–125	9		029	layer, 5G4/1, coarse sandy				
3-2, 148–150	2		030	layer, coarse sandy				
3-5, 94–106	12	100	031	layer, 5GY4/1, sandy	lower Pleistocene	75.48	3.79	
3-6, 97–100	3		032	layer, 5G4/1, very fine grained				
3-6, 102–104	2		033	layer, very fine grained				1.496–1.498
3-6, 117–120	3		034	layer, 5GY4/1, dark gray				
4-3, 129–134	5		035	layer, inclined, 5GY4/1, silty				
4-3, 141–147	6			pocket				
4-4, 12–14	2			pocket, small, 5Y4/1	lower Pleistocene			
4-4, 38–40	2			pod, silt-sized	upper Pliocene			
4-4, 72–76	4			pocket				
4-6, 81–84	3			small pocket				
4-6, 100–105	5		036	layer, arched, very fine-grained, 5GY4/1				
4-6, 113–115	2			pocket				
5-3, 77–85	8	78	037	layer, 5G2/1, fine-grained	upper Pliocene			

TABLE 1 – *Continued*

Sample (Interval in cm)	Thickness (cm)	Smear Slide (cm depth)	Layer Number	Remarks	Age	SiO_2 (%)	ΣFe_2O_3 (%)	Index
Hole 438A (cont.)								
5-3, 103-104	1			pocket, small				
6-2, 71-74	3	74	038	layer, 5GY2/1, silty				
6-3, 72-73	1		039	layer, 5G4/1, very fine grained				
6-3, 85-86	1		040	layer, 5B5/1, medium-grained				
6-3, 123-127	4		041	layer, 5B5/1, silty, graded				
6-3, 148-150	2		042	layer, 5B5/1, very fine grained				
6-4, 17-24	7		043	layer, 5B5/1, medium-grained				1.498-1.499
6-4, 72-73	1			pocket, very fine grained				
7-4, 51-55	4		044	layer, 5Y2.5/1, sandy				
7-4, 71-75	4		045	layer, 5Y7/1, very fine grained				
7-5, 45-51	6	50	046	layer, 2.5YN4/, sandy				
8-4, 98-100	2	100	047	layer, 2.5YN6/, fine-grained				
8-3, 95	>1		048	layer, 2.5YN4/1, medium coarse grained				
8-5, 69-70	1		049	layer, medium-grained				
10-3, 86-88	2	87		pod, 2.5YN2.5/				
11-2, 81-83	2			pocket, 2.5YN2.5/				
11-4, 35-40	5		050	layer, 2.5YN6/, medium-grained	upper Pliocene			
11-6, 0-2			051	layer, 5Y4/2	lower Pliocene			
11-6, 103-105	2			pod, small, 2.5YN3/				
12-1, 65-66	1			pocket, medium-grained, 2.5YN3/				
12-1, 70-71	1			pocket, medium-grained				
12-1, 73-74	1			pocket, medium-grained				
12-1, 87-88	1			pocket, 2.5YN7/, coarse-grained				
12-3, 16-19	3		052	layer, 2.5YN8/, medium-grained	lower Pliocene			
13-3, 35-37	2		053	layer, 2.5YN3/, medium coarse grained				
13-5, 19-24	5		054	layer, 2.5YN8/, medium-grained				
14-2, 11-14	3		055	layer, 5Y8/1				
14-2, 18-22	4		056	layer, inclined, 5Y6/1	lower Pliocene			
14-2, 103-108	5			pocket, 7.5YN6/, fine-grained				
14-3, 7-8	1		057	layer, fine-grained				
14-3, 127	>1		058	layer, fine-grained				
14-4, 42-45	3		059	layer, 2.5YN4/, coarse pumiceous				
14-4, 87-88	1		060	layer, 5Y7/1, fine-grained pumiceous				
14-4, 88-90	2		061	layer, 2.5YN4/, medium-grained pumiceous				
14-4, 117-120	3		062	layer, 2.5YN8/, medium-grained				
16-3, 142-147	5		063	layer, inclined, 2.5YN6/, medium-grained				1.501-1.503
16-4, 0-26	26			pod, thin, elongated downward				
16-5, 86	>1		064	layer, fine-grained, 2.5YN6/				
16, CC, 10	>1		065	layer, 5Y7/1, fine-grained pumiceous				
17-1, 72-75	3	74	066	layer, medium-grained				
17-1, 115-116	1			pocket, fine-grained, 2.5YN7/				
17-1, 117-119	2			pocket, dark gray, silty				
17-2, 145-147	2			pod, very fine grained, gray				
17-2, 147-149	2		067	layer, fine-grained, dark gray				
17-3, 52-54	2		068	layer, 2.5YN9/, silty				1.508-1.511
17-3, 100-104	4	101	069	layer, dark gray				
18-2, 35-40	5	39	070	layer, 2.5YN8/, medium fine grained				
18-4, 27-29	2		071	layer, 7.5YN6/, medium-grained				
18-4, 90-100	10		072	layer, fine-grained, dark gray, 7.5YN3/				
19-3, 93-97	4	96	073	layer, N6., fine-grained				
19-3, 102-105	3	103	074	layer, 5Y3/2, medium-grained, silty				
19-4, 69-72	3		075	layer, N7, fine-grained				
19-5, 31-35	4		076	layer, N5, very fine grained				
20-2, 125-126	1		077	layer, N5, very fine grained				
20-2, 135-137	2		078	layer, N5, fine-grained				
21-1, 6-12	6	9	079	layer, N6, very fine grained				
21-6, 87-88	1		080	layer, N5, very fine grained				
24-1, 52-55	3		081	layer, 5Y3/2, fine-grained, silty				
24-1, 97-101	4		082	layer, N5, very fine grained				
24-1, 125-130	5	127	083	layer, N4, very fine grained				
24-1, 148-150	2		084	layer, sandy, 5Y3/2				
24-2, 0-7	7		084	layer, sandy, 5Y3/2	lower Pliocene			
24-3, 80-82	2		085	layer, N4				
24-4, 57-61	4		086	layer, 5B8/1, silt-sized				
24-6, 83-87	4	85	087	layer, 5Y6/1, very fine grained				
25-3, 34-38	4	35	088	layer, N7, very fine grained				1.501-1.503
25-4, 34-38	4		089	layer, 5Y4/1, silty				
26-2, 11-14	3	11	090	layer, N7, silt-sized				
27-3, 81-83	2	82	091	layer, dark gray, medium-grained sandy				
27-6, 81-88	7	85	092	layer, light gray, graded				1.500-1.504
28-4, 62-65	3			pod, dark gray, silty				
28-4, 141-142	1		093	layer, fine-grained, silty, light gray graded				
29-5, 90-92	2		094	layer, gray, N.7				
30-4, 34-35	1			pocket, light gray				
30-7, 19-21	2			pocket, light gray-white				
31-5, 60-62	2	61	095	layer, silty, 10GY5/2				
32-1, 98-100	2		096	layer, sand-sized, light gray				

TABLE 1 – *Continued*

Sample (Interval in cm)	Thickness (cm)	Smear Slide (cm depth)	Layer Number	Remarks	Age	SiO_2 (%)	ΣFe_2O_3 (%)	Index
Hole 438A(cont.)								
32-1, 141–142	1			pocket, irregular				
32-1, 143–144	1			pocket, very fine grained				
32-1, 145–146	1			pocket, dark gray				
32-2, 15–18	3			pocket, dark gray, medium fine grained				
32-3, 90–93	3	91	097	layer, medium fine grained, light gray, N5				
33-4, 74–75	1	74	098	layer, light gray, N7				
33-5, 141–143	2			pod, mottled, light gray				
33-6, 128–133	5			pocket, pumiceous				
34-3, 84–87	3			pocket, light gray				
34-4, 22–24	2		099	layer, silty, N5				
35-3, 28–30	2	29	100	layer, gray, fine-grained				
35-3, 62–64	2		101	layer, light gray, very fine grained				
35-3, 108–111	3	110	102	layer, 5Y4/2				
35-6, 102–111	9		103	layer, gray, silty, top is chalk	upper Miocene			
36-1, 111–112	1		104	layer, light gray, fine-grained				
36-5, 67–71	4			pocket				
36-6, 8–11	3		105	layer, fine-grained sandy				
36-6, 57–59	2	57	106	layer, fine to medium grained				
40-1, 37–41	4		107	layer, 5B5/1, gray, fine-grained	upper Miocene			
40-2, 9–11	2			pocket, 5G4/1, fine-grained				
42-7, 37–40	3		108	layer, inclined, very fine grained, white				
43-2, 83–85	2			pocket, silty				
43-3, 9–10	1			pocket, 5Y5/1, gray, silty				
43-3, 83–87	4			pocket, 5Y5/1, gray				
44-6, 17–20	3		109	layer, 5YR5/0, dark gray				
45-4, 5–10	5		110	layer, wedge, 5YR4/0, silty				
45-6, 4–17	13		111	layer, inclined, 5Y4/1, silty				
46-5, 5–8	3	7	112	layer, silty, N3, pyritized				
46-5, 86–90	4			pocket, 5YR4/0, dark gray, silty				
50-1, 33–35	2		113	layer				
59-3, 67–70	3	69	114	layer, sandy	middle Miocene			
60-1, 71–73	2	71		pocket, pumiceous				
64-1, 115–117	2	117		5GY4/1, fine-grained, diatomaceous vitreous claystone				
64-3, 27–32	5	30	115	layer, intercalated glauconite, silty				
65-4, 37–45	8			basalt, scoria, clast lappili 5 mm.				
65-4, 105–112	7	110		vitric diatomaceous claystone				
65-5, 10–16	6	13	116	layer, N7, silty				
71-5, 120–125	5	121	117	layer, very fine grained				
73-1, 36–37	1	36	118	layer, thin				
79-6, 85–86	1			pocket				
79-6, 87–89	2			pocket				
84-2, 85–86	1	86		pocket				
Hole 438B								
6-2, 63–66	3	66		pocket, 5B5/1, medium-grained, gray	lower Miocene			
7-2, 87–88	1			pocket				
11-2, 3–4	1			pocket, white, silt-sized				
Hole 439								
5-1, 119–120	1			pod, mottled, silty	middle Miocene			
7-1, 8–10	2		119	layer, inclined, N7, silt-sized	lower Miocene			
7-1, 120–125	5	124	120	layer, inclined, N7, silty				
7-2, 134–140	6		121	layer, inclined, N6, very fine grained				
8-2, 123–127	4		122	layer, N6, very fine grained, cut by normal fault				
8-3, 59–60	>1		123	layer, very fine grained				
8-3, 63–65	>1		124	layer				
8-3, 68–70	2		125	layer, light gray	lower Miocene			
8-3, 78–80	2		126	layer, silty				
8-3, 105–106	>1		127	layer, light gray				
8-4, 41–42	1			pocket, gray				
8-5, 16–17	1			pocket, white, fine-grained, silty				
8-5, 49–51	2			pocket, gray, sandy				
8-5, 98–100	2		128	layer, inclined				
8-6, 98–101	3			pocket, N5, medium-grained				
9-2, 110–115	5			pocket, medium-grained, graded				
9-3, 61–65	4			pocket, 3 pieces, 5B7/1				
9-3, 88–90	2		129	layer, 5B5/1				
9-3, 102–110	8		130	layer, 5B7/1, arched downward, silty				1.501–1.502
9-3, 121–123	2			pocket, white, medium-grained				
9-5, 38–52	14		131	layer, irregular upward 5B5/1, graded				
11-3, 64–71	7		132	layer, 5B5/1, irregular upward				
13-1, 0–17	17			tuffite				
Hole 440								
4-1, 104–112	8	105	001	layer, N3, graded, base 10Y6/2	upper Pleistocene			
4-2, 146–150	4		002	layer, graded, N3-10Y6/2				
4-3, 38–48	10			pod				
4-3, 145–148	3		003	layer, arched upward, N4, mottled				
4-6, 130–134	4		004	layer, graded, N4(b), 5B9/1(t)				

TABLE 1 – *Continued*

Sample (Interval in cm)	Thickness (cm)	Smear Slide (cm depth)	Layer Number	Remarks	Age	SiO_2 (%)	ΣFe_2O_3 (%)	Index
Hole 440 (cont.)								
5-3, 67–75	8			pocket				
5-3, 78–80	2		005	layer, N6, light gray				
5-3, 92–94	2		006	layer, N6, light gray				
6-2, 23–25	2	25	007	layer, N7, silty				
7, CC, 8–15	7		008	layer, N5, very fine grained, sandy				
Hole 440A								
2-3, 135	>1			pocket				
7-1, 86–94	8	86		pocket, 4 pieces, N8, silty				
7-4, 17–18	1	17	009	layer, N6, very fine grained				
7-4, 18–20	2	19	010	layer, N3				
7-5, 58–60	2		011	layer, N3, very fine grained				
Hole 440B								
3-1, 31–33	2	32	012	layer, 5Y6/1, silty				
3-3, 80–81	1			pocket				
5-1, 114–115	1		013	layer, 5Y8/1, with pumice				
5-2, 143–144	1	143	014	layer, N8, silty				
5-6, 133–135	2			pocket, N7, silty				
6-5, 83–86	3		015	layer, 5Y5/3, silty				
7-2, 17–19	2			pocket, N6, silty				
7-4, 6–8	2			pocket, N5, very fine grained				
7-4, 116–118	2			pocket				
10-2, 8–10	2			mottled, N7				
12-5, 21–24	3	22		pocket, N4-N6, with pumice				
13-3, 43–44	1	44		pocket, mottled				
18-1, 118–126	8			pumice accumulated				
23-1, 75–78	3	77	016	layer, N8, very fine grained light gray	upper Pliocene			
30-1, 48–52	4			vitric diatomaceous claystone				
31-1, 140–144				pocket, N6, very fine grained silty				
32-1, 48–50	2		017	layer				
32-2, 18–20	2			pocket, 5Y6/1				
32-3, 87–90	3		018	layer, 5Y6/1				
32-4, 138–146	8		019	layer, inclined, N5, very fine grained				
33-4, 20–25	5		020	layer, inclined				
33-4, 107–110	3		021	layer, inclined, N7				
34-1, 132–134	2		022	layer, N7, silty, mottled				
34-1, 145–147	2	146	023	layer, N7, silty				
34-2, 26–27	1	27	024	layer, N7, very fine grained				
34-2, 97–99	2		025	layer, N8, silty				
34-2, 124–126	2			rocket, N7, fine-grained				
34-3, 82–83	1		026	layer, with pumice				
35-1, 122–123	1		027	layer				
35-1, 140–141	1		028	layer				
35-2, 125–129	4		029	layer, silty				
35-5, 58–62	4		030	layer, 5Y7/1, thick, irregular, silty				
36-2, 121–124	3		031	layer, N8, irregular up and down, silty				
36-3, 23–25	2			pocket, N7, silty				
38-4, 32–42	10			tuffite, 5Y7/3, pale yellow				
39-4, 118–120	2			pocket, N2				
40-3, 92–93	1			pocket, 5Y7/4, fine-grained				
41-1, 81–85	4	81		pocket, N3, silty				
41-1, 144–145	1			pocket, silty				
41-2, 68–69	1			pocket				
41-2, 137–142	5	138		pocket, N3				
43-2, 60	>1			pocket				
43-2, 65–68	3		032	layer, inclined				
43-2, 85–90	5		033	layer, inclined				
45-1, 17–22	5		034	layer, inclined, cut by normal fault, dip 40°				
45-1, 122–126	4			lens of ash, 20° bed				
45-2, 40	>1			pocket				
45-2, 52–53	1			pocket, N6				
46-1, 3–5	2			pocket				
46-1, 132	>1			pocket				
46-1, 140–141	1			pocket				
46-2, 23–24	1			pocket				
46-2, 77–78	1			pocket				
47-1, 102–103	1		035	layer, N5, silty				
48-1, 50–52	2			pocket, N6				
48-1, 68–70	2			pocket, N5, 2 pieces				
48-1, 72–75	3			pocket				
48-2, 75–76	1			pocket, N5				
48-2, 98	>1			pocket, N4				
48-2, 101–102	1			pocket, N4				
48-4, 82–83	1			pocket, N5				
49-1, 71–78	7		036	layer, graded, irregular below				
49-1, 80–82	2			pocket, 2 pieces				

TABLE 1 – *Continued*

Sample (Interval in cm)	Thickness (cm)	Smear Slide (cm depth)	Layer Number	Remarks	Age	SiO_2 (%)	ΣFe_2O_3 (%)	Index
Hole 440B (cont.)								
49-2, 77–87	10		037	layer, 5Y5/2				
49-2, 89–90	1			pocket				
49-2, 91–92	1			pocket				
49-2, 97–100	3			pocket, N5				
49-3, 22–27	5		038	layer, N5, irregular up and down				
49-3, 30–32	2			pocket, 3 pieces				
49-3, 38	>1			pocket				
49-4, 82–83	4			pocket				
49-4, 20	>1			pocket				
49-4, 22–25	3			pocket, N5				
49-4, 37	1			pocket, N6				
50-1, 48–51	3			pocket				
50-1, 73–74	1			pocket, N5				
50-1, 135–137	2			pocket, N5				
51-2, 18–21	3		039	layer, N8, thin, mottled				
51-2, 87–88	1			mottled				
52-1, 20–24	4			pocket, N7				
52-1, 65–76	11			tuffite layer, 5GY6/1				
52-1, 147–148	1			pocket, silty N4				
52-3, 59–63	4		040	layer, N5, nose of fold, silty				
52-3, 70–76	6		041	layer, N5, nose of fold, silty				
54-2, 63–70	7			mottled, cut by fault				
54-2, 82–84	2			pocket				
55-3, 44–47	3			pocket				
55-5, 33–34	>1		042	layer, white calcareous	lower Pliocene			
55-5, 36	>1	36	043	layer, thin				
56-1, 17	>1			pocket				
56-1, 22	>1			pocket				
56-1, 48–50	2		044	layer, bioturbation				
56-1, 80	>1	80		pocket				
56-2, 44–51	7		045	layer, 5GY6/1, tuffite				
58-1, 135–137	2			pocket, N6	upper Miocene			
58-5, 134–135	1		046	layer, irregular				
59-1, 38–40	2		047	layer, N7				
59-3, 86–88	2		048	layer, N5, arched downward				
60-1, 108–110	2			pocket, N7				
60-2, 53–55	2		049	layer				
60-2, 78–81	3		050	layer				
60-2, 108–110	2		051	layer				
60-4, 25–27	2		052	layer, 5Y7/1				
61-1, 100–102	2			pocket, N8				
61-1, 120–126	6	123		vitric clast layer, N4				
63-3, 5–9	4		053	layer, N7, silty				
63-3, 57–59	2		054	layer, 5Y6/1				
63-3, 63–67	4	63	055	layer, 5Y6/1				
63-4, 90–92	2		056	layer				
64-2, 65–68	3			pocket				
64-2, 140–148	8		057	layer, inclined				
Hole 441								
2-2, 95–97	2	96		pocket, 5Y5/3, clay-sized				
2-4, 55–57	2			pocket, 5Y4/3, silty				
2-5, 42–43	1	42		pocket, 5Y3/2, very fine grained				
2-5, 77–82	5			layer, 5Y7/1, silty				
2-5, 86–96	10	95		layer 5Y7/1, silty				
7, CC, 19–20	1			mottled, N8, very fine grained silty				
Hole 441A								
2-1, 0–12				tuffite, 5Y4/1, graded				
11-1, 70	>1			pod				
11-1, 126	>1			pod				
H-1-3, 99–101	2	99		layer, inclined, N8, mottled, dip 15°				
H-1-4, 24–27	3	25		layer, inclined, silt-sized				
H-1-4, 48–51	3			pocket				
H-4-2, 75–80	5	76		layer, inclined, silty				
Hole 441B								
1-1, 83–99	16			layer, 5Y6/1, N7, light olive				
1-1, 109–120	11	113		layer				
H-1-4, 20–32	12	23		pocket				
Hole 436								
1-2, 18–21	3	21	001	layer, N9-N7	Pleistocene			
1-2, 82–85	3	82	002	layer				
1-3, 103–105	2	105		pocket				
1-4, 20	>1			pocket				
1-4, 109–111	2	110		pocket				

TABLE 1 – *Continued*

Sample (Interval in cm)	Thickness (cm)	Smear Slide (cm depth)	Layer Number	Remarks	Age	SiO_2 (%)	ΣFe_2O_3 (%)	Index
Hole 436 (cont.)								
1-4, 128–142	14	133		pocket				
1-5, 14–20	6			pocket				
1-5, 39–46	7			pocket				
1-5, 81–87	6	87		pocket				
1-5, 100–112	12			pocket				
3-1, 16–20	4	17		pocket				
3-4, 70–84	14	80		pocket				
3-5, 32–37	5			pocket				
3-5, 80–82	2	80		pocket				
3-5, 90	>1			pocket				
4-1, 82–83	2			pocket				
4-1, 148–150	2			pocket				
4-2, 2–6	4	4		pocket				
4-4, 88–90	2			pocket				
4-6, 20–23	3			pocket				
5-2, 68–80	12	78		pocket				
5-3, 69–73	4							
6-2, 33–57	14			patch				
6-2, 132				patch				
6-3, 108–139	31			patch				
6-4, 0–50	50			patch				
6-4, 80–90	10			patch				
6-5, 59–62	3			patch				
7-1, 70								
7-2, 5–								
7-2, 15–20								
7-2, 25–30								
7-2, 37								
7-2, 73								
7-2, 85				patch	Pleistocene			
7-2, 98–104								
7-2, 108								
7-2, 115								
7-4, 65–92								
7-5, 135–150								
7-6, 25								
7-6, 60								
8-1, 30								
8-1, 73								
8-1, 140–143	3		003	layer				
8-2, 39				patch				
8-2, 120								
8-3, 0–40	40	24	004	layer, light gray in upper, 5YR6/1 in lower				
8-3				patch				
8-4								
8-5								
9-1, 19–30	11	25	005	layer, basaltic				
9-2, 20–40			006	layer, N6-5G2/1				
9-2, 72–93	21	84	007	layer				
9-5				pocket, basaltic				
9-5				pocket, basaltic				
9-6				pocket, basaltic				
9-6				pocket, basaltic				
10-1, 32–36	4		008	layer, pocket				
10-1, 50–68	18	67	009	layer				
10-1, 84–90	6		010	layer				
10-3				pocket				
10-4				pocket				
10-5				pocket				
11-2				pocket				
11-3, 0–4			011	layer				
11-4				patch				
11-4, 41–56	15		012	layer				
11-4				pocket	upper Pliocene			
11-4				pocket				
11-6, 49–55	6		013	layer				
12-4				pocket				
12-4				pocket				
12-4				pocket				
12-4, 93–133	40	95, 128	014	layer				
12-6, 1–10	9		015	layer				
13-4								
13-5, 0–10	10		016	layer				
14-1, 11–12	1		017	layer				
14-1								

TABLE 1 – *Continued*

Sample (Interval in cm)	Thickness (cm)	Smear Slide (cm depth)	Layer Number	Remarks	Age	SiO_2 (\$)	ΣF_2O_3 (%)	Index
Hole 436 (cont.)								
14-1								
14-2, 51–60	9	58	018	layer				
14-3								
14-3, 60–66	6		019	layer				
14-3, 111–115	4		020	layer				
14-4								
15-6, 105–150	45	115	021	layer, N7	lower Pliocene			
15-7, 0–10	10		022	layer, N7				
16-3, 99–110	11	100	023	layer, 5GY4/2				
16-4								
16-4								
16-6								
16-6								
17-1								
17-1								
17-3, 50–60	10	55	024	layer				
17-3								
17-3, 99–110	11		025	layer				
17-3								
17-3								
17-4								
17, CC								
19-4, 63–72	9		026	layer				
20-1					lower Pliocene			
20-1, 130–140	10	139	027	layer				
20-2, 15–25	10	17	028	layer				
21-1								
22-1, 75–84	9	80	029	layer				
22-1, 112–117	5		030	layer				
23-1, 30–40	10		031	layer				
23-1, 47–50	3		032	layer				
23-1, 75–76	1		033	layer				
23-2, 10–16	6		034	layer				
23-2, 27–33	6		035	layer				
23-2, 70–73	3		036	layer				
23-2, 100–102	2		037	layer				
23-3, 130–140	10	138	038	layer				
23-4, 20–26	6							
23-5								
27-1, 82–84	2		039	layer	upper Miocene			
27-2, 81–86	5		040	layer				
27-3, 6–10	4		041	layer				
29-1, 67–73	6	70	042	layer				
29-1, 112–120	8	118	043	layer				
30-1, 42–50	8		044	layer				
30-1, 56–61	5		045	layer				
30-1, 98–104	6		046	layer				
30-1								
30-1								
30-3, 80–86	6		047	layer				
31-1, 33–40	7		048	layer				
31-5, 11–12				layer				
33-1								
33-2, 73–80	7	77	050	layer				
33-2								
33-5								
33-6, 112–120	8	113	051	layer, graded				
34-3, 19–25	6							
34-5, 30–37	7		052	layer	upper Miocene			
35-3, 21–30	9	28	053	layer				
36-4, 112–122	10	118	054	layer	middle Miocene			
36-4								
36-4								
36-5								
36-6, 28–32	4	33	055	layer				
37-2								
37-2								
37-2								
37-3								
38-2, 26–31	5		056	layer				
38-2								
38-4, 16–20	4		057	layer				
38-7								

DSDP cores. In the present study, we define distinct ash layers as traceable ones and number them from top to bottom. Cadet and Fujioka (this volume) obtained a frequency curve of the volcanicity with geologic time by using the visual core description. They considered all ash layers and small pods or pockets as a record of volcanism, although small pods or pockets seem not to correlate among sites.

The curve obtained by Cadet and Fujioka shows a large, broad peak in the Pliocene and a small peak at the boundary between the lower and the middle Miocene at Sites 438 and 439, whereas two definite separated peaks are observed in the upper and the lower Pliocene at Site 440, at the trench slope bench. Although the curve at Site 440 has a double peak, the two curves at 438 and 439 and at 440 are quite similar. The double peak at Site 440 may be caused by sedimentation rate, bottom topography, current, degree of bioturbation, and many factors other than volcanic activity itself.

At Site 436, volcanic materials increase upward from Miocene to Recent. Furuta and Arai (this volume) counted the numbers of the volcanic ash layers and ashy pods or pockets and found that at Site 436 there were 56 volcanic ash layers and pods in the Pleistocene, 31 in the late Pliocene, 27 in the early Pliocene, 20 in the late Miocene, and 12 in the middle Miocene. The estimated frequency curve is different from that of the upper slope sites. The difference in number of ash layers on the oceanic plate is due to its continuous movement toward the Japanese Islands, which enables the volcanic glass gradually to reach Site 436. Meanwhile, Sites 438, 439, and 440 are fixed relative to the Japanese Islands. It is very interesting to compare the two environments, oceanic plate and continental. Precise study of Leg 56 volcanic ash is necessary.

Smear Slide Observation

Smear slide observation carried out onboard shows a continuous downhole variation in volcanic glass content dispersed in sediment and sedimentary rock. In Unit 1 of Sites 438 and 439, vitric volcanic glass composes up to 10 per cent of the sediment, then gradually decreases downward. At the boundary between the upper and middle Miocene, this component seems to disappear; however, in the lower Miocene it again increases gradually, often exceeding 10 per cent. In the lower Miocene, volcanic glass dispersed in sediment reaches a maximum content and rarely exceeds 20 per cent of the constituents in Lithologic Unit 3.

Lithologic Unit 3 (von Huene et al., 1978) consists of sandy claystone and diatomaceous claystone throughout, showing deep bathyal sedimentary environment. Burrow mottling, microfaults, and fractures are common. The vitric component of sediments has a plateau of approximately 20 per cent throughout Units 3 and 4, then gradually decreases downward and disappears in Units 5, 6, and 7. The frequency pattern in dispersed volcanic glass correlates well to that in volcanic ash layers and small pods or pockets. However, at Site 440, volcanic glass dispersed in sediments is not so variable throughout Holes 440, 440A, and 440B. At this site, volcanic glass content always reaches 5 per cent or more, with slight local fluctuations. The frequency pattern of dispersed volcanic ash which distinguishes between the two sites is due to the sedimentation rate, topography, current, bioturbation, and many other factors in the depositional environment.

Smear slide observation shows volcanic glass to be predominately rhyolitic, with an almost transparent white appearance—quite different from the brown basaltic glass with a high refractive index which occurs sporadically throughout the sedimentary section. Nor is this rhyolitic glass representative of the predominant rhyolitic volcanism in the source region. This aspect will be discussed in the following section.

Petrography of Volcanic Glass

Table 2 presents a description of volcanic ash—type, color, and grain size—and shows the refractive index of volcanic glass and its constituent minerals. Experimental procedures are as follows: First, tephra samples are cleaned by an ultrasonic cleaner. Clay minerals and other dusts smaller than 5 μm are sieved off with water. Next constituent minerals, type, color, and grain size of volcanic glass shard are examined under the microscope. Refractive indices are measured by the phase-contrast technique, using monochromatic illumination at a controlled constant room temperature of 24 ± 0.2°C. The margin of error of the indices of immersion liquid is less than ± 0.0002. The measured results are summarized by the maximum and minimum values of refractive indices in the tephra sample, the mean range in which more than 80 per cent of the measured refractive indices are concentrated, and the most frequent values of the refractive indices. Volcanic glass is usually separated into two types, pumice and bubble wall. Usually both types occur in the same ash layer. Figure 1 shows electron microscope photographs of volcanic glass samples in which large, tabular pumice predominates. These glasses were impregnated with an epoxy resin and prior to chemical analysis with an electron-probe microanalyzer. The maximum grain size of volcanic glass varies from 2.5 mm to 0.04 mm, from very coarse sand to silt-size. The very coarse grained glass probably derives from a nearby source, whereas fine-grained glass probably has a more distant source. The settling velocity of volcanic glass was investigated by Fisher (1965), who demonstrated that bubble wall glass has a slightly higher rate of settling velocity than pumice, given a similar grain size.

Refractive indices of volcanic glass range from 1.496 to 1.529, corresponding to a rhyolitic to rhyodacitic composition. A bimodal refractive index is observed in one ash layer.

Recently, Yoshikawa (1978) investigated the volcanic glass in the Osaka Group (Pliocene) and discussed the relative between refractive indices and the SiO_2 and Fe_2O_3 content of volcanic glass. In acidic volcanic glass, the relationship is not clear. Data from Leg 57 shows no clear relationship either. Examination of the relationship between refractive index and chemical composition is necessary.

TABLE 2
Description and Refractive Index of Volcanic Glass

1	2	3	4	5	6	7	8	9	10
438-2-5, 109-110	0.4	+	Pl+, Mf-	Fib Str Bw	Cl	1.502-1.506			
438-3-7, 96-97	1.0	++	Pl++, Ho Hy Au Mt	P	Cl Wh	1.503-1.520	1.502-1.505		76.45
438-7-7, 3-4	2.0	+++	Pl+++, Hy Au Mt	Spg Str	Wh Cl	1.500-1.506	1.504+ 1.515-1.520	1.504+ 1.518+	
438-8-7, 11-12	1.0	++	Pl++, Hy Au Mt	Fib Str	Wh Cl	1.501-1.504	1.502-1.504		75.48
438-10-3, 124-125	1.8	+++	Pl+++, Hy Au Mt	Spg Fib	Wh Cl	1.504-1.506		1.503+	77.40
438-10-5, 80-81	0.6	+++	Pl+++, Ho Hy Au Mt	Spg Fib	inc rich	1.503-1.505		1.505+	76.35
438-11-4, 85-86	0.1	+	Pl++ (Px+)	P B	Cl Wh	1.506-1.508		1.504+	78.21
438A-1-1, 70-72	0.3			Spg	Cl	1.506-1.510			
438A-2-4, 132-133	0.5	+++	Pl++, Hy Au Mt	Fib	Cl	1.500-1.502			74.08
438A-2-5, 20-21	0.5-0.6	++	Pl++, Hy Au Mt	P	Cl	1.502-1.503			78.41
438A-3-5, 94-96	1.5	++	Pl++, Ho Hy Au	Fib Str	Inc rich	1.504-1.506		1.505+	
438A-3-6, 101-102	0.5	++	Pl++, Bi Hy Au Mt	P	Cl	1.496-1.498		1.497+	75.48
438A-6-4, 22-23	0.6-0.7	++	Pl+++ Ho(Cum) Bi Mt	P	Cl	1.498-1.499			
438A-14-4, 43-44	1.2	+++	Pl++, Hy Au Mt	Fib Spg	Cl	1.506-1.509		1.508+	
438A-16-3, 143-145	0.5		Mt+	P B	Cl	1.501-1.503		1.502+	76.30
438A-17-3, 52-54	1.0	+	Pl++, Hy Au Mt Ho	P	Wh	1.508-1.511		1.510+	
438A-19-3, 95-96	0.5	+++	Pl+++, Hy Au Mt	Fib	Cl	1.500-1.502		1.501+	
438A-25-3, 36-37	0.4-0.5		Ho Mt+	P B	Cl	1.501-1.503			
438A-27-3, 83-84	2.0	++	Pl+, Hy Au lith +	Spg	Wh	1.520-1.529	1.526-1.529	1.502+	73.02
438A-27-6, 86-87	1.0	+	Pl+, lith	P B	Cl	1.500-1.504	1.501-1.503	1.502+	
438A-33-6, 119-120	1.0	++	Pl++, (Hy Au Mt)	P	Wh	1.508-1.511		1.509+	
438A-34-1, 53-54	1.5		lith.++	Fib Spg	Wh	1.501-1.505			76.45
438A-45-4, 8-9		+++	Pl, Ho Mt						
438A-50-5, 115	2.5	+	Pl+, Mf-	Spg Fib	Wh	1.504-1.506		1.505+	
438B-3-5, 94-96	1.0	+++	Pl++, Hy Ho Mt Au	P	Wh			(1.506+)	
438B-9-3, 5-20			Pl++, Cum Bi Mt						
439-9-3, 105-108	0.04	+	Pl+ (fine)		Cl	1.501-1.502		1.5015+	

Note: 1 = sample number, interval in cm; 2 = maximum grain size; 3 = amount of free crystal; 4 = mineral composition; 5 = type of volcanic glass; 6 = color of volcanic glass; 7 = range of refractive index; 8 = mean range of refractive index; 9 = mode of refractive index; 10 = SiO_2 content of volcanic glass (in %, measured with electron-probe microanalyzer). Abbreviations: + = poor, ++ = moderate, +++ = abundant, Pl = plagioclase, Ho = hornblende, Hy = hypersthene, Mt = magmetite, Px = pyroxene, Bi = biotite, Au = augite, lith = lithic, Mf = mafic mineral, Cum = cummingtonite, Fib = fibrous, Str = striped, Spg = spongy, P = pumice type, B = bubble wall type, Cl = clear, Wh = white, inc = inclusion.

Tephra Correlation

Several investigators have successfully correlated deep sea tephra layers with source volcanic rocks on land (Ninkovich, 1968; Ninkovich & Shackleton, 1975; Keller et al., 1978). Although deep sea tephra is several hundred or more km from the source volcanic rocks, it is correlatable using diagnostic features of volcanic ash. Bowles et al. (1973) succeeded in correlating ash layers with the reflected horizons of a 3.5-kHz echogram off the coasts of Guatemala and Costa Rica. Leg 57 sites are located at about 200 to 300 km east of the Quaternary volcanic front on land, and frequent occurrence of many ash layers and ashy pods or pockets in Leg 57 sites produces fruitful correlations. Although volcanic glass at these sites shows very similar features downward throughout the cores, the drilling disturbance, post depositional tectonic disturbance, and bioturbation present serious problems. It was possible to correlate only two layers between Holes 438 and 438A, several hundred meters apart. From the point of view of biostratigraphy sedimentation rate, Samples 438-7-2, 48–50 cm and 438-7-2, 103–105 cm may be reliably correlated with Sample 438A-5-3, 77–85 cm and with the ashy pods beneath this layer. Samples 438-3-6, 91–98 cm and 438A-2-2, 122–129 cm are also correlatable. Furuta and Arai (this volume) correlated the two uppermost ash layers in Hole 436 with the uppermost ones obtained during *Hakuho-maru* cruise KH77-1. In the area of Sites 438, 439, 440, and 441 the uppermost sediments consist of such coarse-grained sand and pebbles that it was very difficult to obtain perfect cores. Two ash layers may be correlated with each other by chemical composition of glass and biostratigraphical age: Samples 438-11-5, 26–32 cm and 438A-6-4, 17–24 cm.

II. MINERALOGY

Table 2 shows the constituent minerals, as well as other features, of volcanic glass in ash layers. The constituent minerals observed are plagioclase, hornblende, hypersthene, augite, biotite, and magnetite. Cummingtonite occurs only rarely. Plagioclase is the most abundant, which is typical of rhyolitic volcanic rocks. Other constituent minerals vary from layer to layer. Chemical analyses were carried out with an electron-probe microanalyzer (see Tables 3–6). Table 3 shows the chemical composition of plagioclase in selected layers. It ranges from $An_{73.43}$ in Sample 438A-24-1 to $An_{7.57}$ in 438A-3-6, 101–102 cm. Volcanic glass contains an average of 70 per cent SiO_2. High calcium plagioclase coexists with very acidic volcanic glass. From their study of the Tarumae volcano, Katsui et al. (1978) demonstrated that the bulk composition was intermediate whereas the liquid was very acidic and had erupted under conditions of very high vapor pressure.

Table 4 shows the chemical composition of pyroxene to be Wo-En-Fs. Clinopyroxene is augite and orthopy-

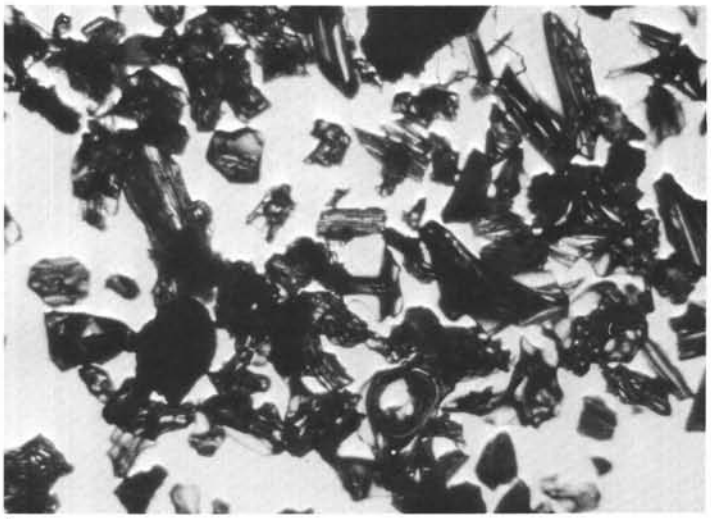

A

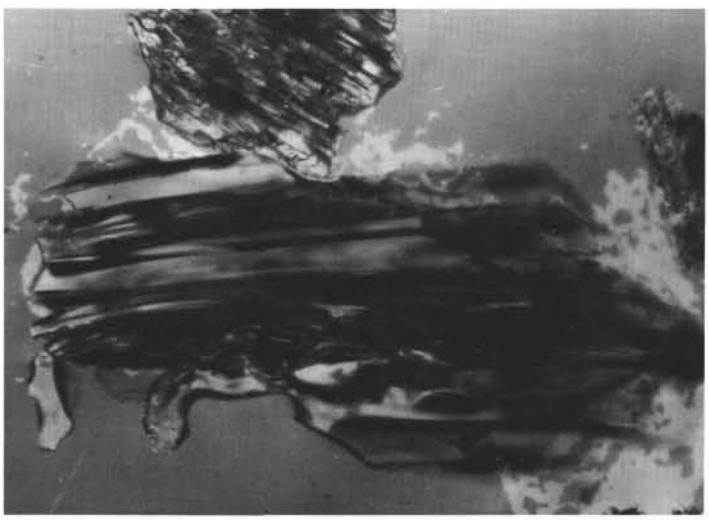

B

C

Figure 1. *Microscopic photographs of volcanic glass.* A. *Sample 438A-6-3, 125–126 cm;* B. *Sample 438A-2-5, 109–110 cm;* C. *Sample 438A-6-3, 125–126 cm, typical pumice-type glass with small vesicles.*

TABLE 3
Chemical Composition of Plagioclase (%)

Sample	438-7-7, 3 cm	438-10-3, 124 cm	438-11-1, 41 cm	438-11-5, 30 cm	438A-2-2		438A-3-6, 101 cm	438A-6-2, 72 cm			438A-19-3, 95 cm
		Core			Core	Core		Core	Rim		
An	40.98	62.59	44.63	69.11	45.97	49.30	7.57	52.43	47.06	43.24	40.09
Ab	58.26	36.80	54.21	27.52	53.37	50.20	38.29	46.46	51.93	53.31	58.46
Or	0.76	0.61	1.17	3.37	0.66	0.50	54.14	1.11	1.02	1.45	1.44

roxene is hypersthene and ferrohypersthene. The range of chemical composition in zoned pyroxenes is very narrow.

Hornblende and biotite were also analyzed (Tables 5 and 6). The hornblendes and biotites are chemically homogeneous.

Fisher (1965) investigated the settling velocity of volcanic ash. He demonstrated that glass shards of different types settle at a velocity considerably lower than that of quartz grains. Based on their benthonic foraminiferal assemblages (von Huene et al., 1978), an outer shelf environment was inferred for the sedimentary section in the lower Miocene in Units 5 and 6; a shallow bathyal depth was inferred for Unit 4; and a deep bathyal environment was inferred throughout Units 2 and 3. Therefore it is possible that some volcanic shards are not deposited together with crystals of the same magma.

III. CHEMICAL COMPOSITION OF VOLCANIC GLASS

In order to estimate the nature of volcanic activity in the source region of each tephra layer, chemical analyses were carried out with a Model JXA-5 electron-probe microanalyzer, following the experimental procedures of Nakamura and Kushiro (1970). Volcanic ash samples are softly crushed and then cleaned with an ultrasonic cleaner. Glass is separated from its constituent minerals with a heavy liquid. Both glass and constituent minerals are respectively impregnated with an epoxy resin, then ground and polished with diamond paste for about three hours.

These conditions proved severe for labile glass. Because the alkali element count decreased with exposure to the electron beam, the beam was defocused. Variation in the experimental conditions gives slightly different values for the chemical composition of the glass. Thus total amount of oxide components ranges from about 85 per cent to 100 per cent. We were unable to pinpoint the amount of volatile material in each volcanic glass grain. A conventional examination was made of volcanic ash. Heating at 110°C and at 1050°C gives a rough idea of ignition loss. The preliminary result revealed a total ignition loss of 5.92 per cent for Sample 438A-16-3, 143–145 cm. To estimate the volume more precisely, we consulted the data of other investigators. Yoshikawa (1978), who reported the chemical composition of volcanic glass in the Osaka Group, found that the H_2O content in 24 upper Pliocene volcanic glasses ranges from 3.78 per cent to 5.59 per cent by weight. Because the similarity of chemical composition of the volcanic glass between the Osaka Group and the Japan Trench area, it may be correct to regard the H_2O content of rhyolitic glass as about 5 weight per cent. The chemical composition of obsidian and pitchstone is also very similar to that of rhyolitic volcanic glass (Kawano, 1950). Pitchstone always has a slightly higher H_2O content than obsidian. Yoshikawa's result seems to accord well with pitchstone with regard to H_2O content. In our study the low total oxide content of the glass may be due to hydration and/or to the experimental conditions. The hydration of volcanic glass is an important factor presently under investigation.

General Remarks on the Chemical Composition of Volcanic Glass

About 350 chemical analyses of volcanic glass were carried out with an electron-probe microanalyzer. Smith and Westgate (1969) and Westgate and Fulton (1975) performed such analyses, but many problems about the experimental conditions are still unsolved. Chemical composition of selected volcanic glass is listed in Table 7. SiO_2 content ranges from 64 per cent to 80 per cent corresponding to that of dacite to rhyolite. These values are very similar to those of obsidian and pitchstone (Kawano, 1950). Samples often exceed 75 per cent SiO_2, but this value seems slightly high compared with the other volcanic rocks. The Al_2O_3 content varies from about 10 per cent to 15 per cent, the average being 11 per cent. This value is similar to the volcanic rocks with the same SiO_2 content. TiO_2 content is a good means of distinguishing one ash layer from the other (Czamanske and Porter, 1965; Yokoyama, 1972). TiO_2 content varies from 0.03 per cent to 0.65 per cent among the ash layers. Fe_2O_3 (total iron) and MgO vary considerably in different samples. The FeO*/MgO ratio is also quite variable. In some samples, this ratio exceeds 100. MnO is a minor constituent but distinct nevertheless layer by layer. CaO, Na_2O, and K_2O content changes a great deal both in the original magmatic process and in the hydration process of volcanic glass. During crystallization, the growth of plagioclase changes the CaO, Na_2O, and K_2O ratios of the magma. K_2O content varies greatly, showing a maximum of about 5 per cent.

SiO_2–(Na_2O + K_2O)

The chemical composition of the volcanic glass determined by electron-probe microanalysis is plotted in a SiO_2–($Na_2O + K_2O$) diagram proposed by Kuno (1966) in order to discover if the glass belongs to a alkalic or nonalkalic rock series. In this diagram, only water-free

TABLE 3 – *Continued*

438A-24-1		438A-33-4, 73 cm			438A-40-1		439-9-3, 105 cm		439-9-5, 49 cm		
		Core	Rim				Core	Core			Rim
73.43	20.39	28.54	40.03	37.74	30.61	31.26	60.06	39.56	50.04	41.35	36.66
26.35	77.53	69.38	58.53	60.70	68.07	66.74	39.13	59.01	49.06	56.39	60.50
0.23	2.08	2.08	1.44	1.56	1.33	2.00	0.18	1.43	0.89	2.24	2.84

TABLE 4
Chemical Composition of Pyroxene (%)

Sample	438-10-3, 124 cm		438-11-1, 41 cm			438A-2-2				438A-6-2, 72 cm				438A-33-4, 73 cm
	Cpx Core	Cpx Rim	Cpx Core	Opx Core	Rim	Opx Core	Rim	Opx Core		Core	Rim	Opx Core	Opx Rim	Opx
Wo	44.33	43.93	40.76	2.70	2.83	2.65	3.55	2.46	2.84	2.15	2.66	2.54	2.93	26.09
En	40.36	39.99	39.17	58.70	58.45	65.15	65.08	45.56	46.80	47.07	45.63	45.72	44.81	44.21
Fs	15.31	16.09	20.07	38.60	38.73	32.20	31.37	51.97	50.36	50.78	51.71	51.74	52.25	29.70

Note: Cpx = clinopyroxene, Opx = orthopyroxene.

TABLE 5
Chemical Composition of Hornblende (%), Sample 438A-24-1, 98–99 cm

	Core	Rim
SiO_2	45.862	46.390
TiO_2	0.528	0.486
Al_2O_3	7.533	7.233
Fe_2O_3	13.658	13.285
MnO	0.245	0.345
MgO	13.778	14.660
CaO	11.473	11.821
Na_2O	1.700	1.607
K_2O	0.528	0.575
Total	95.305	96.402
Ca	27.78	27.76
Mg	46.41	47.89
Fe	25.81	24.35

data were plotted. Most of the data fall in low total alkali areas—that is, in the nonalkalic rock series. Some hydrated glass falls in the alkalic rock series, and the alteration or hydration of the glass is critical for its classification. Nevertheless, the trend of most volcanic glass is low alkalic—that is, nonalkalic rock series, whether calc-alkalic or tholeiitic (Figure 2).

FeO^*-(Na_2O + K_2O)-MgO

All the data are plotted in the FAM (iron-alkali-magnesium) diagram proposed by Wager and Deer (1939) (Figure 3). Although the data disperse in this diagram, most plots are along the F–A axis, which suggests that most of the volcanic glass belongs to the tholeiitic rock series represented by the Skaergaard trend. The most FeO^*-(total iron as FeO) enriched sample is plotted near the FeO^* corner of the Skaergaard trend. Generally, acidic volcanic glass is enriched in alkali compared with FeO^* and MgO. In this diagram

TABLE 6
Chemical Composition of Biotite (%)

	438A-3-6, 101–102 cm	Recalculated Composition [a]	438A-3-6, 101–102 cm Core	Recalculated Composition [a]	Rim	Recalculated Composition [a]
SiO_2	35.224	5.9686	33.301	5.8228	34.914	5.9547
TiO_2	3.421	0.4359	3.262	0.4289	3.429	0.4398
Al_2O_3	15.642	3.1237	15.626	3.2201	15.425	3.1005
Fe_2O_3*	17.329	2.4556	17.018	2.4885	17.184	2.4510
MnO	2.223	0.3190	2.222	0.3291	2.342	0.3384
MgO	10.557	2.6667	10.661	2.7790	10.747	2.7324
CaO	0.020	0.0037	0.041	0.0076	0.010	0.0019
Na_2O	0.473	0.1556	0.426	0.1444	0.433	0.1431
K_2O	9.093	1.9656	8.877	1.9801	8.872	1.9301
Total	93.982	17.0943	91.435	17.2006	93.356	17.0919

[a]Number of ions of each element (not oxide) recalculated on the basis of 24 oxygen atoms.

TABLE 7
Chemical Composition of Selected Volcanic Glass (%)

Layer No.	1	10	23	32	37	55	119	78	93	109	130	127
Sample	438-	438-	438-	438-	438-	438A-	438A-	438A-	438A-	438A-	438A-	438A-
(Interval in cm)	2-5, 109	7-7, 3-4	8-7, 11-12	10-3, 124-125	10-5, 80-81	1-1, 70-72	2-4, 132-133	3-5, 94-96	3-6, 101	5-3, 81	6-2, 72	6-3, 125-126
SiO_2	76.446	75.475	77.396	76.345	78.208	74.081	78.410	75.48	74.662	78.027	74.080	74.519
TiO_2	0.218	0.184	0.137	0.294	0.241	0.429	0.210	0.19	0.173	0.232	0.148	0.049
Al_2O_3	11.136	11.366	11.403	10.407	11.343	12.910	11.391	11.38	11.830	11.155	11.496	11.633
Fe_2O_3*[a]	2.055	1.472	1.479	1.316	1.366	3.078	1.188	3.97	1.377	1.151	1.256	1.711
MnO	0.114	0.092	0.137	0.034	0.076	0.218	0.173	0.07	0.102	0.010	0.000	0.161
MgO	0.238	0.197	0.154	0.217	0.192	1.774	0.125	0.32	0.190	0.173	0.110	0.058
CaO	2.101	1.521	1.436	1.439	1.557	3.873	1.210	0.82	1.275	1.214	1.134	0.972
Na_2O	0.485	2.244	2.050	2.195	2.069	1.615	1.856	0.97	0.941	0.920	1.562	1.967
K_2O	0.886	1.417	1.852	2.905	2.101	0.963	2.292	1.08	1.658	1.803	2.728	3.008
Total	93.679	93.968	96.044	95.151	97.153	98.942	96.854	94.28	92.208	94.684	92.515	94.076
FeO**[b]	1.850	1.325	1.331	1.184	1.229	2.770	1.069	3.573	1.239	1.036	1.130	1.540
Al_2O_3/SiO_2	0.146	0.151	0.147	0.136	0.145	0.174	0.145	0.151	0.158	0.143	0.155	0.156
FeO**[b]/MgO	7.771	6.725	8.644	5.458	6.403	1.562	8.554	11.166	6.523	5.988	10.276	26.550
CaO/Na_2O	4.332	0.678	0.700	0.656	0.753	2.398	0.652	0.845	1.355	0.132	0.726	0.494
K_2O/Na_2O	1.827	0.631	0.903	1.323	1.015	0.596	1.235	1.113	1.762	1.989	1.746	1.529
$Na_2O + K_2O$	39.64	70.63	72.43	78.45	74.58	36.20	77.65	34.49	64.52	69.25	77.58	75.69
FeO**[b]	53.48	25.56	24.71	18.21	21.98	38.89	20.01	60.12	30.76	26.35	20.43	23.43
MgO	6.88	3.80	2.86	3.34	3.43	24.91	2.34	5.38	4.72	4.40	1.99	0.88
CaO	60.51	29.35	26.90	22.01	27.19	60.04	22.58	28.57	32.91	30.84	20.91	16.34
Na_2O	13.97	43.30	38.40	33.57	36.13	25.03	34.64	33.80	24.29	23.37	28.80	33.08
K_2O	25.52	27.34	34.69	44.43	36.69	14.93	42.78	37.63	42.80	45.80	50.29	50.58
$Na_2O + K_2O$	1.46	3.90	4.06	5.36	4.29	2.61	4.28	2.17	2.82	2.88	4.64	5.29
SiO_2	81.60	80.32	80.58	80.24	80.50	74.87	80.96	80.06	80.97	82.41	80.07	79.21

[a] Fe_2O_3* = total iron calculated as Fe_2O_3.
[b] FeO** = total iron calculated as FeO.

one volcanic ash sample obtained in one layer is higher in MgO than other samples. This shows that it is composed of several volcanic glasses with different chemical compositions. Two possibilities suggest themselves: one is that several eruptions of different volcanoes in the source region may take place at almost the same time and that their chemical compositions are slightly different. The second possibility is that several eruptions of the same volcano may take place within a very short time span and the degree of magma differentiation may be slightly different. In the present case, the two possibilities are equally important.

In Figure 4, two different ash layers which may be correlated with each other are tested for three components: FeO*, MgO, and total alkali. Therefore the correlation of each ash layer is more reliable than if the refractive index alone were used. At the same time, the three additional components, CaO, Na_2O, and K_2O, are useful indicators for distinguishing the layers. Figure 4 shows the relationship between two different layers, Sample 438-11-5, 30–31 cm and Sample 438A-6-4, 22–23 cm. In this figure, A shows the FeO*–MgO–($Na_2O + K_2O$) relationship and B the K_2O–CaO–Na_2O relationship. It is clear from this diagram that the two samples have the same chemical composition. Biostratigraphic results support this evidence. Both ash layers belong to the upper Pliocene, and ratios FAM and CaO–Na_2O–K_2 are concentrated in very narrow and overlapping areas. Thus it is valid to correlate the two layers with each other.

This method of correlation is more reliable than other methods and is quite useful for surrounding areas, such as the Northeast Japan Arc, which supply similar volcanic ash materials. In northern Honshu, the famous upper Pliocene Shirakawa dacite is widely distributed. The correlation of the two aforementioned tephra layers with the Shirakawa dacite of similar age remains for future investigation.

As stated earlier, the chemical composition of the volcanic glass is quite similar to that of obsidian and pitchstone. Fresh obsidian and pitchstone are plotted in the diagram in Figure 5. The data of all the volcanic glass show a close genetic similarity.

IV. DISCUSSION

As stated in the previous sections, the frequency curve derived from the number of ash layers constitutes a record of the volcanicity near the Japan Trench sites. The land volcanism of the Tohoku region of Honshu has been summarized by many investigators (Sugimura et al., 1963; Kuno, 1966; Horikoshi, 1976). Figure 6 shows Horikoshi's estimation of volcanic activity in the Tohoku arc from approximately 30 m.y.B.P. to Recent. In the Quaternary, the volume of volcanic rocks is large near the volcanic front and is mainly tholeiitic in composition, becoming more alkalic as it moves west of the front. This relationship was well summarized by Kuno (1966) in many other circum-Pacific arcs. Moreover, the volume of volcanic activity in the Tertiary is four times that of the Quaternary. According to Horikoshi's es-

TABLE 7 – *Continued*

115 438A- 6-4, 22–23	139 438A- 14-4, 43–44	146 438A- 17-3, 52–54	160 438A- 19-3, 95–96	164 438A- 24-1, 98	172 438A- 24-4, 60	179 438A- 24-6, 85	185 438A- 27-3, 83–84	199 438A- 33-6, 119–120	211 438A- 34-1, 53–54	221 438A- 40-1, 39	233 438A- 50-5, 115	243 438B- 9-3, 5–6	253 439- 7-1, 125
75.879	76.300	74.15	75.914	72.470	75.94	77.83	73.023	74.33	76.447	73.022	74.046	75.39	74.221
0.135	0.327	0.19	0.103	0.080	0.08	0.15	0.367	0.30	0.097	0.109	0.114	0.06	0.543
11.514	11.208	12.12	13.299	11.482	11.52	11.59	13.434	11.67	11.412	11.688	12.287	11.90	15.231
0.630	2.292	4.63	1.322	1.221	1.97	1.12	1.737	4.30	1.579	1.388	1.596	1.96	3.184
0.103	0.073	0.08	0.079	0.072	0.07	0.04	0.095	0.11	0.075	0.034	0.205	0.01	0.213
0.070	0.282	0.30	0.092	0.102	0.16	0.14	0.203	0.29	0.023	0.119	0.128	0.08	0.511
0.547	1.942	1.13	1.232	1.000	2.12	1.03	3.555	1.15	1.025	1.350	1.636	0.30	2.679
2.852	1.090	1.87	1.130	2.395	0.50	1.03	3.397	0.80	2.100	2.400	2.534	0.79	0.290
4.117	1.868	1.07	2.628	2.315	1.26	2.52	1.386	1.60	1.672	2.815	1.681	3.07	1.543
95.847	95.382	95.54	95.798	91.136	93.59	95.44	97.196	94.56	94.432	92.924	94.227	93.57	98.415
0.567	2.063	4.167	1.190	1.099	1.773	1.01	1.563	3.87	1.421	1.249	1.436	1.764	2.866
0.152	0.147	0.163	0.175	0.158	0.152	0.149	0.184	0.157	0.149	0.160	0.166	0.158	0.205
8.100	7.315	13.890	12.933	10.774	11.081	7.200	7.701	13.345	61.787	10.497	11.222	22.050	5.608
0.192	1.782	0.604	1.090	0.418	4.240	1.000	1.047	1.438	0.488	0.563	0.646	0.380	9.238
1.444	1.714	0.572	2.326	0.967	2.520	2.447	0.408	2.000	0.796	1.173	0.663	3.886	5.321
91.63	55.78	39.69	74.56	79.68	47.66	75.56	73.03	36.59	72.32	79.22	72.94	67.67	35.18
7.54	38.90	56.26	23.61	18.59	48.01	21.46	23.87	58.99	27.24	18.97	24.85	30.93	55.01
0.92	5.32	4.05	1.83	1.73	4.33	2.98	3.10	4.42	0.44	1.81	2.21	1.40	9.81
7.28	39.63	27.76	24.69	17.51	54.64	22.49	42.64	32.39	21.37	20.56	27.96	7.21	59.38
37.95	22.24	45.95	22.65	41.94	12.89	22.49	40.74	22.54	43.78	36.56	43.31	18.99	6.43
54.78	38.12	26.29	52.67	40.54	32.47	55.02	16.62	45.07	34.86	42.88	28.73	73.80	34.20
7.27	3.10	3.08	3.92	5.17	1.88	3.72	4.92	2.54	3.99	5.61	4.47	4.13	1.86
79.17	79.99	77.61	79.24	79.52	81.14	81.55	75.13	78.61	80.95	78.58	78.58	80.57	75.42

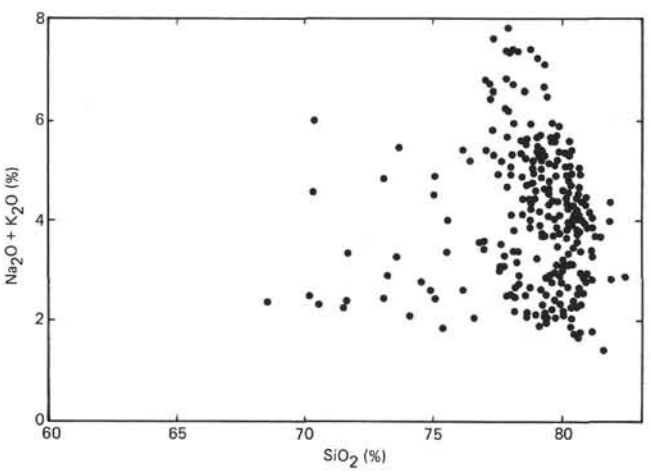

Figure 2. *Alkali–silica diagram of volcanic glass from Leg 57. Components are recalculated water-free.*

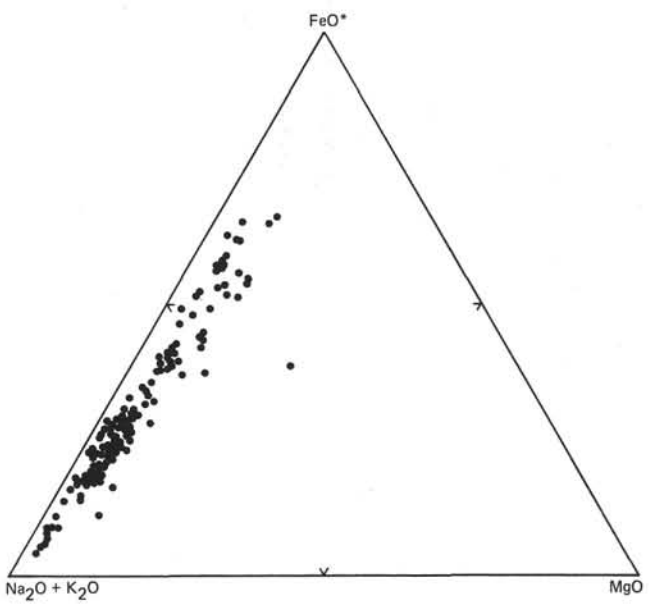

Figure 3. *FeO*–($Na_2O + K_2O$)–MgO diagram of volcanic glass. FeO* represents total iron calculated as FeO.*

timate, the amount of volcanic rock in his "Initial Stage" (27 m.y.B.P.–13 m.y.B.P.) is greater than that of his "Stational Stage" (after 13 m.y.B.P.). Horikoshi's estimate and that of Cadet and Fujioka differ in that land volcanicity is very intense during the Miocene, whereas it is intense at the Japan Trench sites during the Pliocene. This discrepancy is due mainly to the fact that volcanic activity at DSDP sites reflects the more explosive acidic rhyolitic ash, so that the curve obtained by Cadet and Fujioka shows only acidic volcanism and contains no basic volcanic products.

The factors controlling the mode of eruption are very complicated (Verhoogen, 1955; Aramaki, 1975). One of these is the chemical composition of magma (Katsui et al., 1978). Generally, acidic magma contains more volatile components than basaltic magma. Rhyolitic volcanic glass seems to be more widely distributed than

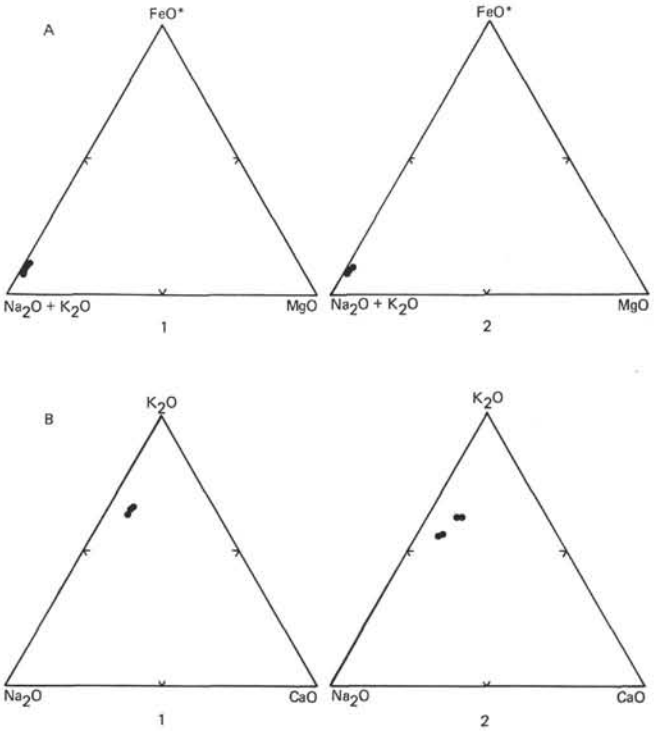

Figure 4. *A triangle plot of correlation of two ash layers.* 1. *Sample 438-11-5, 30–31 cm;* 2. *Sample 438A 6-4, 22–23 cm;* A. *FeO*–($Na_2O + K_2O$)–MgO diagram;* B. *K_2O–Na_2O–CaO diagram.*

basaltic glass. For example, Ninkovich (1968) correlated deep sea ashes with those on land in the New Zealand Taup-Rotorua area. In his data on acidic and basic tephra, volcanic glass distribution depends mainly on its chemical composition. Acidic volcanic glass is often found more than 1000 km from the source (Machida and Arai, 1976).

As stated earlier, basaltic glass at DSDP sites is rare compared with rhyolitic glass. Further correlation between on land and deep sea tephra in the Tohoku arc is necessary, and the frequency curve of volcanicity needs revision.

The chemical composition of volcanic glass discussed in Section III has been obtained from fairly fresh samples. However, most of the volcanic glass had suffered from hydration and/or alteration to various degrees. Some of the basaltic glass observed in smear slides had been altered to palagonite. Also, in some rhyolitic glass, very weak birefringence shows up under the microscope. Glass samples were examined by X-ray diffractometer, revealing a broad peak of clay minerals. Alteration of glass shards is the most severe problem in determining magma type. Chemical scanning patterns in Figure 7, A and B show the Ca–Kα, Fe–Kα, and Mg-Kα relationships in a single grain of volcanic glass. Sample 438A-33-6, 119–120 cm has a homogeneous pattern throughout the grain, whereas 438B-9-3, 5–6 cm has a heterogeneous pattern. In the latter case, Ca, Mg, and Fe decrease near the periphery of the grain, forming a regular chemical gradient, and Si, Al, and Fe decrease uniformly near the vesicle. This may indicate secondary leaching of the cation toward the rim. These chemical scanning patterns are valid means of determining the hydration and/or alteration processes of the volcanic glass.

The K_2O, Na_2O, and CaO relationships of many volcanic glasses were examined, and several examples were shown in Figure 5. The K_2O/Na_2O ratio of volcanic glass seems to increase toward the rim of the grain, but not in all cases. A similar trend was observed by Moore (1966) in the glass samples of altered pillow lavas. His results show clearly the increase of K_2O content as hydration increases. The K_2O/Na_2O ratio of each kind of volcanic glass is variable. The K_2O/Na_2O ratio in sea water is very small compared with the same ratio in the glass. We can therefore assume that leaching of K_2O/Na_2O, if it does take place, depends not on fresh sea water but on interstitial water.

Recently, Hein et al. (1978) investigated the diagenesis of volcanic ash recovered during DSDP Leg 19 in the

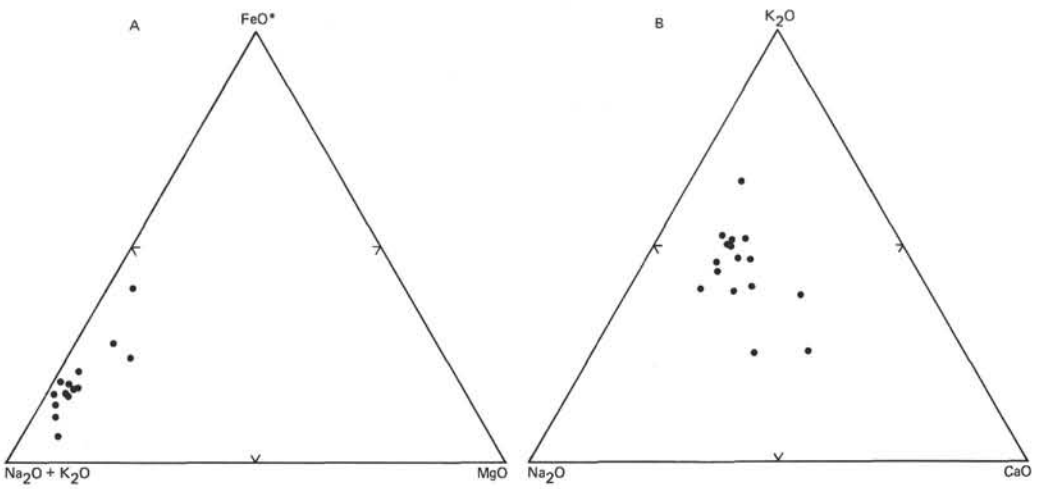

Figure 5. *Ternary diagrams for Japan obsidian and pitchstone. (Data from Kawano, 1950; diagrams same as in Figure 4.)*

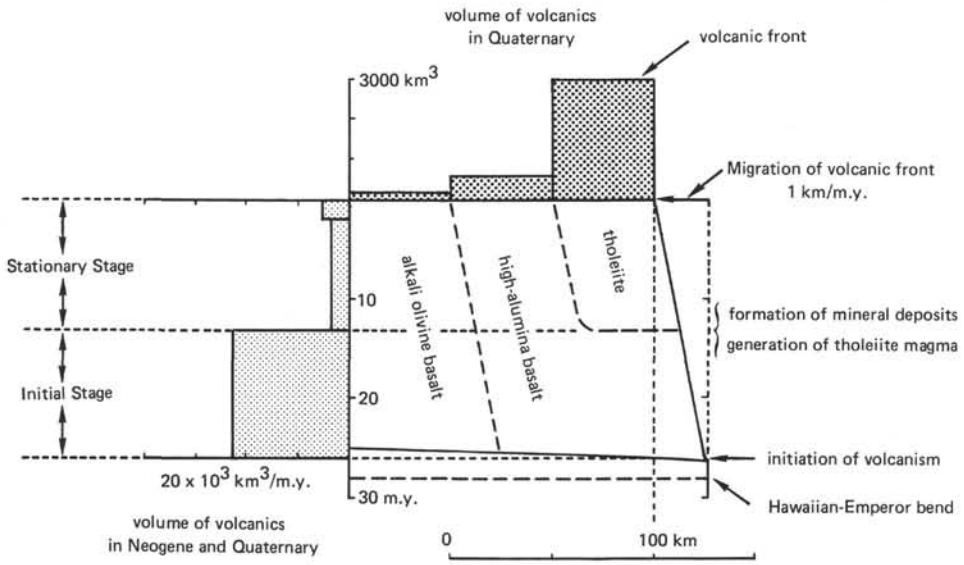

Figure 6. *Modal volume of volcanic rocks in the Tohoku Arc, Japanese Islands. (From Horikoshi, 1976.)*

Bering Sea. Downhole temperature measurement at Leg 19 sites indicates 40°C or less at the bottom and an isotopic temperature, measured by oxygen, of 70°C. However, at Site 439, bottom temperature is less than 29°C and observed alteration seems very weak compared with that of Leg 19.

Settling velocity of volcanic glass and mafic minerals are critical to determining the magmatic conditions of eruption. Fisher (1965) investigated the settling velocity of various types of glass using Stoke's law. If his results are valid, settling velocities of mafic heavy minerals and glass of the same radii are considerably different. Whether or not mafic minerals coexist with groundmass glass is a critical question which requires an answer in the near future.

SUMMARY

1) Explosive acidic volcanism took place with the greatest intensity during the Pliocene, judging from the volcanic ash layers of Leg 57.

2) Three volcanic ash layers were correlated from the standpoint of biostratigraphy and chemical composition.

3) The chemical composition of the volcanic glass shows that in the SiO_2–($Na_2O + K_2O$) diagram it belongs in the nonalkalic rock series and that in the FeO*–($Na_2O + K_2O$)–MgO diagram it exhibits trends similar to those of a tholeiitic rock series.

4) The K_2O/Na_2O ratio of the slightly hydrated volcanic glass increases toward the rim in a single grain of glass. This trend is very similar to the palagonitization reported by many investigators.

ACKNOWLEDGMENTS

The authors would like to express sincere thanks to Drs. Noriyuki Nasu, H. Kagami, K. Kobayashi, J. Segawa, H. Tokuyama, and T. Ishii for their valuable suggestions and critical reading of this manuscript.

REFERENCES

Aramaki, S., 1975. Classification and mechanism of volcanic eruptions. *Bull. Volcanol. Soc. Jpn. Ser. 2,* 20, 205–221.

Bowles, F. A., Sack, R. N., and Carmichael, I. S. E., 1973. Investigation of deep-sea volcanic ash layers from equatorial Pacific cores. *Geol. Soc. Am. Bull.,* 84, 2371–2388.

Czamanske, G. K., and Porter, S. C., 1965. Titanium dioxide in pyroclastic layers from volcanoes in the Cascade Range. *Science,* 150, 1022–1025.

Fisher, R. V., 1965. Settling velocity of glass shards. *Deep Sea Res.,* 12, 345–353.

Hein, J. R., and Scholl, D. W., 1978. Diagenesis and distribution of late Cenozoic volcanic sediment in the southern Bering Sea. *Geol. Soc. Am. Bull.,* 89, 197–210.

Hein, J. R., Scholl, D. W., and Miller, J., 1978. Episodes of Aleutian ridge explosive volcanism. *Science,* 199, 137–141.

Horikoshi, E., 1976. Development of late Cenozoic petrogenic provinces and metallogeny in Northeast Japan. *Geol. Assoc. Can. Spec. Pap.,* 14, 121–142.

Katsui, Y., Oba, Y., and Saya, T., 1978. Records of volcanic eruptions in historic times and estimation of future eruptions. *Bull. Volcanol. Soc. Jpn. Ser. 2,* 23, 41–52.

Kawano, J., 1950. Natural glasses in Japan. *Rep. Geol. Surv. Jpn.,* 137. (In Japanese with English abstract).

Keller, J., Ryan, W. B. F., Ninkovich, D., and Altherr, R., 1978. Explosive volcanic activity in the Mediterranean over the past 200,000 yrs as recorded in deep sea sediments. *Geol. Soc. Am. Bull.,* 89, 591–604.

Kennett, J. P., and Thunell, R. C., 1975. Global increase in Quaternary explosive volcanism. *Science,* 187, 497–503.

Kuno, H., 1966. Laterial variation of basaltic magma type across continental margins and island arcs. *Bull. Volcanol. Soc. Jpn. Ser. 2,* 29, 195–222.

Machida, H., and Arai, F., 1976. The very widespread tephra —The Aira-Tn ash. *Science,* 46, 339–347. (In Japanese)

Moore, J. G., 1966. Rate of palagonitization of submarine basalt adjacent to Hawaii. *U.S. Geol. Surv. Prof. Pap.,* 550-D, 163–171.

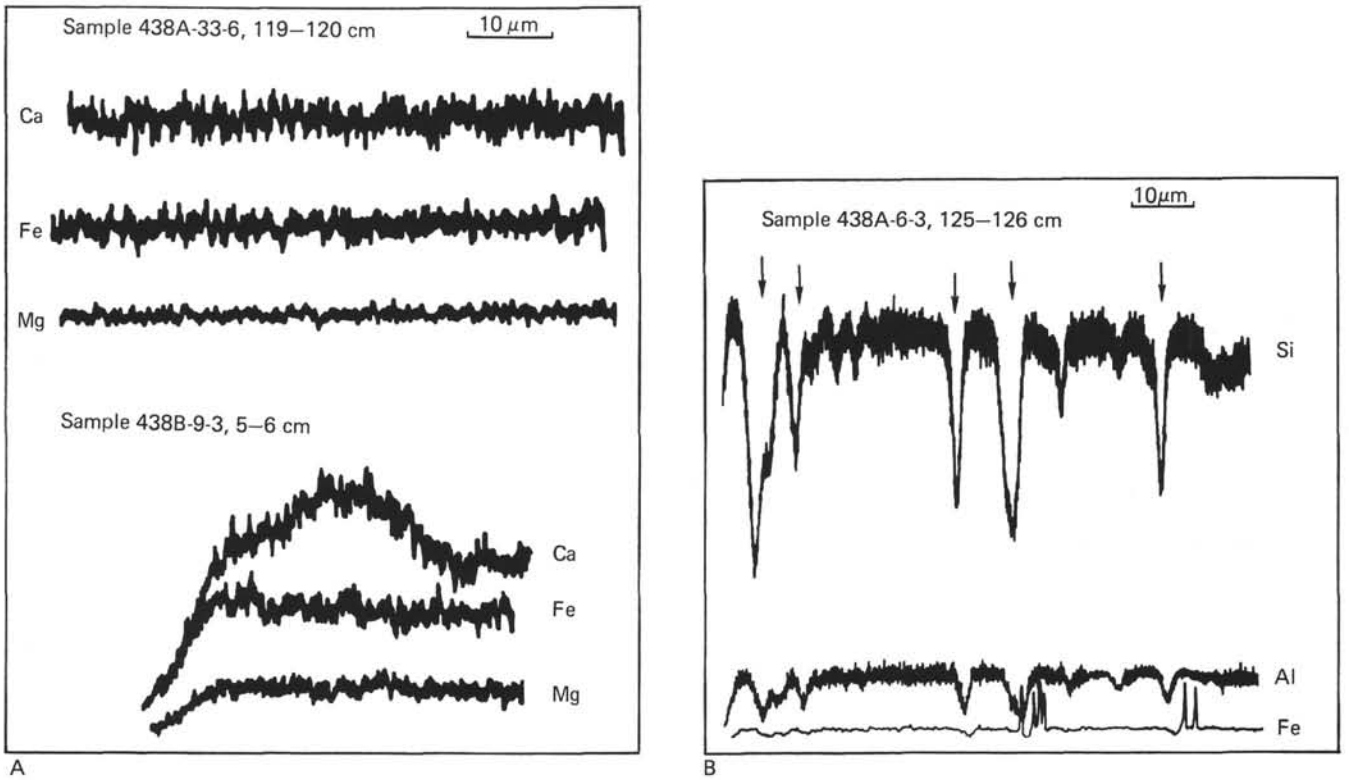

Figure 7. *Chemical scanning pattern of volcanic glass shard.* A. *Ca–Mg–Fe relation. The upper sample shows a homogeneous pattern; the lower shows remarkable variation from core to rim within a single volcanic glass grain.* B. *Si–Al–Fe relation. Si and Fe decrease gradually toward the vesicles.*

Nakamura, Y., and Kushiro, I., 1970. Compositional relations of coexisting orthopyroxene, pigeonite and augite in a tholeiitic andesite from Hakone Volcano. *Contr. Mineral. Petrol.*, 26, 265–275.

Ninkovich, D., 1968. Pleistocene volcanic eruptions in New Zealand recorded in deep-sea sediments. *Earth Planet. Sci. Lett.*, 4, 89–102.

Ninkovich, D., and Donn, W. L., 1976. Explosive Cenozoic volcanism and climatic implications. *Science,* 194, 899–906.

Ninkovich, D., and Shackleton, N. J., 1975. Distribution, stratigraphic position and age of ash layer "L" in the Panama Basin region. *Earth Planet. Sci. Lett.*, 27, 20–34.

Smith, D. G. W., and Westgate, J. A., 1969. Electron probe technique for characterizing pyroclastic deposits. *Earth Planet. Sci. Lett.*, 5, 313–319.

Sugimara, A., Matsuda, T., Chinzei, K., and Nakamura, K., 1963. Quantitative distribution of late Cenozoic volcanic materials in Japan. *Bull. Volcanol. Soc. Jpn., Ser. 2,* 26, 125–140.

Verhoogen, J., 1955. Mechanics of ash formation. *Am. J. Sci.*, 249, 729–739.

von Huene, R., Nasu, N., Fujioka, K., et al., 1978. Japan Trench transected. *Geotimes,* 23, 16–21.

Wager, L. R., and Deer, W. A., 1939. The petrology of the Skaergaard intrusion, Kangerdlugssuaq, east Greenland. *Med. Groen.*, 105 (No. 4).

Westgate, J. A., and Fulton, R. J., 1975. Tephrostratigraphy of Olympia interglacial sediments in south-central British Columbia, Canada. *Can. J. Earth Sci.*, 12, 489–502.

Yokoyama, T., 1972. Discrimination of the volcanic ash layers by means of the features of the volcanic glass, with special reference to the difference of the titanium contents in the volcanic glass of the Plio-Pleistocene Osaka Group, Japan. *Jpn. Assoc. Quat. Res.*, 11, 247–253.

Yoshikawa, S., 1978. Chemical composition of glass in volcanic ash layers of the Osaka Group. *J. Geol. Soc. Jpn.*, 84, 131–140.